

Photochemical Competence of Assembled Photosystem II Core Complex in Cyanobacterial Plasma Membrane*

Received for publication, September 7, 2004, and in revised form, November 17, 2004
Published, JBC Papers in Press, December 15, 2004, DOI 10.1074/jbc.M410218200

Nir Keren, Michelle Liberton, and Himadri B. Pakrasi‡

From the Department of Biology, Washington University, St. Louis, Missouri 63130

Cyanobacterial cells have two autonomous internal membrane systems, plasma membrane and thylakoid membrane. In these oxygenic photosynthetic organisms the assembly of the large membrane protein complex photosystem II (PSII) is an intricate process that requires the recruitment of numerous protein subunits and cofactors involved in excitation and electron transfer processes. Precise control of this assembly process is necessary because electron transfer reactions in partially assembled PSII can lead to oxidative damage and degradation of the protein complex. In this communication we demonstrate that the activation of PSII electron transfer reactions in the cyanobacterium *Synechocystis* sp. PCC 6803 takes place sequentially. In this organism partially assembled PSII complexes can be detected in the plasma membrane. We have determined that such PSII complexes can undergo light-induced charge separation and contain a functional electron acceptor side but not an assembled donor side. In contrast, PSII complexes in thylakoid membrane are fully assembled and capable of multiple turnovers. We conclude that PSII reaction center cores assembled in the plasma membrane are photochemically competent and can catalyze single turnovers. We propose that upon transfer of such PSII core complexes to the thylakoid membrane, additional proteins are incorporated followed by binding and activation of various donor side cofactors. Such a stepwise process protects cyanobacterial cells from potentially harmful consequences of performing water oxidation in a partially assembled PSII complex before it reaches its final destination in the thylakoid membrane.

Photosystem II (PSII)¹ is an integral membrane chlorophyll-protein complex that is a part of the photosynthetic electron transfer chain in the thylakoid membranes of cyanobacteria and plant chloroplasts. PSII catalyzes the extraction of electrons from water and the production of oxygen. The electrons are transferred to plastoquinones through a series of redox active cofactors (1). On the electron acceptor side, a pheophytin molecule accepts an electron from the reaction center P₆₈₀ chlorophyll assembly. The electron is transferred to the Q_A quinone and finally to the Q_B quinone. On the donor side, the

oxidized P₆₈₀ extracts an electron from the D1-Yz tyrosine, which in turn extracts an electron from the manganese cluster. Each reaction cycle requires the absorption of four photons to complete the oxidation of two water molecules, produce one di-oxygen molecule, and reduce two plastoquinones (1).

The photosystem II structure as resolved during recent x-ray crystallographic studies contains 19 protein subunits, 7 carotenoids, 2 hemes, 1 non-heme iron, two pheophytins, and 36 chlorophylls (2). Central to the function of PSII are the D2 and D1 proteins that bind one pheophytin molecule each and form the Q_A and Q_B binding sites of the acceptor side of PSII, respectively. In addition, both D1 and D2 participate in the coordination of the P₆₈₀ chlorophyll assembly at the heart of PSII. The Mn₄-Ca-Cl cluster that catalyzes water oxidation on the donor side of PSII is coordinated by amino acid residues in the D1 and CP43 proteins (2). The donor side complex is stabilized by as many as five extrinsic proteins (3).

Assembly of PSII is a continuous process in oxygenic photosynthetic organisms, since the radical photochemistry performed by PSII exposes its proteins to photooxidative damage (4). The redox potential of P₆₈₀ is the highest measured in any biological system (1). PSII proteins in general and the reaction center core D1 protein in particular turn over constantly (4). Notably, the degradation of the D1 protein is accelerated under high light intensities but takes place even under very low light intensities (5).

The PSII assembly process is tightly regulated to ensure the correct stoichiometric ratio of its numerous components (6). Apart from the protein subunits, chlorophylls, hemes, non-heme iron, and the manganese cluster are assembled into the mature structure. Precise control of the assembly process is required to avoid oxidative damage from partially assembled PSII centers with redox cofactors. The assembly of the manganese cluster, for example, is timed by the cleavage of the carboxyl-terminal extension of the precursor form of the D1 protein (pD1) by the CtpA protease (7).

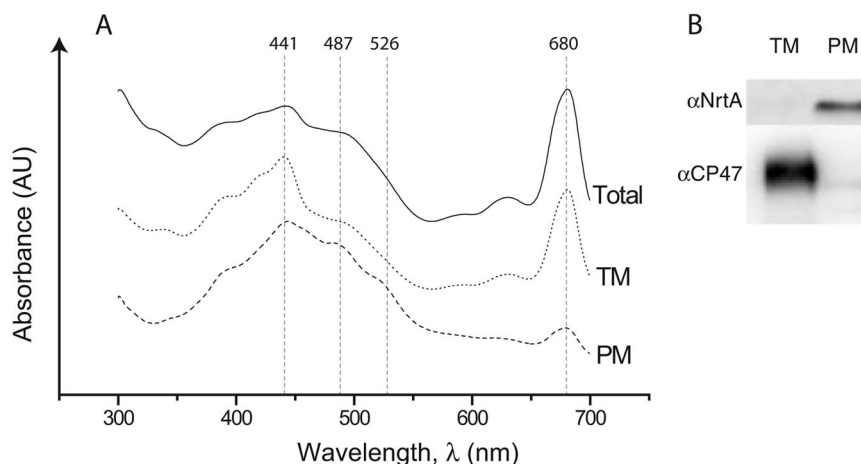
In our studies on the assembly pathway of PSII in cyanobacteria we took advantage of the polymer two-phase partitioning technique (8). Using this technique we separated pure plasma membranes (PM) and thylakoid membranes (TM) from the cyanobacterium *Synechocystis* sp. PCC 6803. In a previous study we reported the existence of a number of PSII and PSI proteins in the PM (8). In particular, PM contains the core D1, D2, and cytochrome *b*₅₅₉ subunits but not the peripheral CP43 and CP47 subunits of PSII. Furthermore, PSII proteins in the PM were shown to be present in a chlorophyll-protein assembly. Based on these findings, we suggested that the PSII core complex is assembled in PM. In this communication we provide evidence for the activity of PSII in PM and suggest a topological model for the sequence of events that takes place in the pathway of PSII assembly in a cyanobacterial cell.

* This work was supported by the Department of Energy (to H. B. P.). The costs of publication of this article were defrayed in part by the payment of page charges. This article must therefore be hereby marked "advertisement" in accordance with 18 U.S.C. Section 1734 solely to indicate this fact.

‡ To whom correspondence should be addressed. Tel.: 314-935-6853; Fax: 314-935-6803; E-mail: Pakrasi@wustl.edu.

¹ The abbreviations used are: PSII, photosystem II; PM, plasma membranes; TM, thylakoid membranes; Chl, chlorophyll; DCMU, 3-(4-dichlorophenyl)-1,1-dimethylurea.

FIG. 1. Isolation of plasma and thylakoid membranes from *Synechocystis* cells. A, absorption spectra of isolated total membrane, TM, and PM fractions. Spectra are base-line-shifted for clarity. B, immunodetection of NrtA and CP47 proteins in isolated TM and PM fractions.



EXPERIMENTAL PROCEDURES

Bacterial Cell Culture Conditions—*Synechocystis* 6803 cells were grown in BG11 medium (9) at 30 °C under 50 $\mu\text{mol photons m}^{-2} \text{s}^{-1}$ white light. Large volume (3–4 liters) cultures were grown with vigorous bubbling with humidified air. Cells were harvested by centrifugation after 5–7 days of growth, frozen in liquid nitrogen, and stored at –80 °C.

Membrane Isolation and Two-phase Partitioning—Frozen cells were thawed on ice and resuspended in a low salt buffer (20 mM potassium phosphate, pH 7.8). Cells were broken in a 50-ml bead beater (Bio Spec, Bartlesville, OK) using 0.17–0.18-mm glass beads. Membranes were collected as described previously (10). The total membrane pellet was resuspended and homogenized in the two-phase buffer (0.25 M sucrose, 5 mM potassium phosphate, pH 7.8). Two-phase systems were prepared from stock solutions of 20% (w/w) Dextran T-500 (Amersham Biosciences) and 40% (w/w) polyethylene glycol 3350 (Sigma). 3.75 g of total membranes were added to each polymer mixture, resulting in 5.8%, 10-g polymer systems (10). The tubes were shaken vigorously and placed on ice. Partitioning was performed by centrifugation at $6,700 \times g$ for 10 min in a fixed angle rotor. Upper and lower phases were collected and repartitioned with new lower and upper phases, respectively. The separation procedure was repeated four times for each top and bottom phase. Throughout the procedure the tubes were kept on ice and in darkness to avoid photodamage.

Protein Separation and Immunodetection—Membrane proteins were separated by SDS-PAGE (3 M urea, 16%). Samples were loaded on an equal protein (30 $\mu\text{g/sample}$) basis. For immunodetection, proteins were blotted onto nitrocellulose, incubated with specific antisera, and visualized by chemiluminescence (West Pico, Pierce).

Spectroscopy—UV-visible spectroscopy was performed using a DW2000 spectrometer (SLM-AMINCO, Urbana, IL). Chlorophyll concentration was measured in methanol extracts for the membrane fractions (11). 77 K fluorescence spectrum was measured on a FluoroMax-2 fluorometer (Jobin Ivon, Longjumeau, France). Fluorescence kinetics were measured on an FL100 apparatus (Photon System Instruments, Brno, Czech Republic). Measurements were performed on an equal chlorophyll basis (16 μg of Chl/ml). Samples were dark-adapted for 3 min before measurement. Manganese concentrations in isolated membranes digested in 5% nitric acid were measured using an AA600 atomic absorption spectrometer (PerkinElmer Life Sciences).

Radioactive Herbicide Binding—Radioactive ^{14}C -labeled 3(3,4-dichlorophenyl)-1,1-dimethylurea (DCMU) was obtained from Amersham Biosciences. 1-ml samples containing 25 μg of Chl were incubated with radioactive DCMU in the presence or absence of a 0.1 mM excess cold DCMU. The samples were incubated in the light for 10 min. Then the membranes were sedimented by centrifugation ($195,000 \times g$ for 10 min). The concentration of the radioactive DCMU in the medium was measured by scintillation counting as described in Lind *et al.* (12). The ratio of the radioactivity measured in the presence and absence of cold DCMU was used to calculate the concentrations of bound and free [^{14}C]DCMU.

RESULTS

To dissect the function of PSII complexes from purified PM and TM membranes, we have modified the protocol for such membrane isolation (10). The original two-dimensional proto-

col required an overnight sucrose gradient centrifugation step. The long preparation time reduces the photochemical activity of the isolated membranes. Instead, we used the polymer two-phase isolation step and omitted the overnight sucrose gradient centrifugation step. The result is a faster procedure, ~5 h long. The yield of this procedure on a chlorophyll basis is typically around 12%. The overall color of purified PM is orange. This color is a result of absorption typical of carotenoids in the 450 to 550-nm range (Fig. 1A). The dominant chromophore in TM was chlorophyll, evident from the absorption at 440 and 680 nm (Fig. 1A). Nevertheless, chlorophyll could be detected in PM (Fig. 1A). The chlorophyll content of PM was 1/10 that of TM on a protein basis (Table I). Although the ratio of chlorophyll to protein in PM was low, its concentration did not fluctuate considerably in the five independent preparations analyzed during the current study (Table I). As markers for the purity of the isolated membranes, we have identified the NrtA and CP47 proteins that are found exclusively in PM and TM, respectively (8). In our modified preparations, NrtA was not detected in TM, and CP47 could hardly be detected in PM, indicating that the membrane fractions are highly purified (Fig. 1B). Therefore, the chlorophyll detected in PM cannot be a result of TM cross-contamination.

To determine whether the chlorophyll present in the purified membrane fractions is functionally assembled, we measured its fluorescence characteristics. In the 77 K fluorescence spectra of isolated TM, a dominant peak at 720 nm was observed (Fig. 2). This peak is a result of photosystem I (PSI) fluorescence (8). In our previous study, PM-localized PSI core complexes were detected. In addition, such complexes were shown to be capable of light-induced charge separation (8). We have also detected emission peaks at 695 and 684 nm, which are ascribed to fluorescence from PSII. In comparison, in PM a number of major differences were detected. Two new peaks appeared at 673 and 682 nm. A 684-nm peak was not detected, and the 695-nm peak was present as a shoulder of the dominant 682-nm peak. A similar fluorescence spectrum containing blue-shifted peaks was observed in isolated D1-D2-cytochrome b_{559} PSII core complexes (13). The 682-nm peak was ascribed to the P_{680} chlorophyll assembly, and the 673-nm peak was ascribed to unassembled chlorophyll. To verify that the 673-nm peak is truly a result of chlorophyll fluorescence, we measured the excitation spectrum for this wavelength. Indeed, such an excitation spectrum closely resembled the absorption spectrum of chlorophyll (data not shown).

Photosynthetic electron transfer activity at room temperature was assayed by measuring time-resolved chlorophyll fluorescence kinetics (14). Overall, PM exhibited three times

TABLE I
Properties of thylakoid and plasma membranes

Chl/protein ratio is based on five independent preparations. Manganese concentrations were measured by atomic absorption spectroscopy ($n = 3$). The 682/692-nm fluorescence ratio (Fig. 2) is based on four independent measurements. The rate of fluorescence rise is calculated as the area above the fluorescence curve between 0 and 0.5 s ($n = 3$). Due to the large difference in F_o values, the curves were normalized to $F_m - F_o$ as shown in Fig. 3, A and B. Binding of DCMU in PM and TM membranes was measured by displacement of [14 C]DCMU by nonradioactive DCMU. The concentration of bound [14 C]DCMU was derived from the fraction of [14 C]DCMU released by the addition of nonradioactive herbicide. Total amounts of [14 C]DCMU were 734 pmol/mg of Chl.

	TM	PM
Chl/protein ($\mu\text{g}/\text{mg}$)	81 ± 15	7.1 ± 1.2
Mn/Chl (mol/mol)	0.05 ± 0.03	0.23 ± 0.05
682/692-nm fluorescence ratio	1.002 ± 0.105	1.51 ± 0.27
Fluorescence rise kinetics, area above the curve (absorbance units)	213 ± 23	85 ± 9
Bound [14 C]DCMU (pmol/mg of Chl)	120.8	116.8

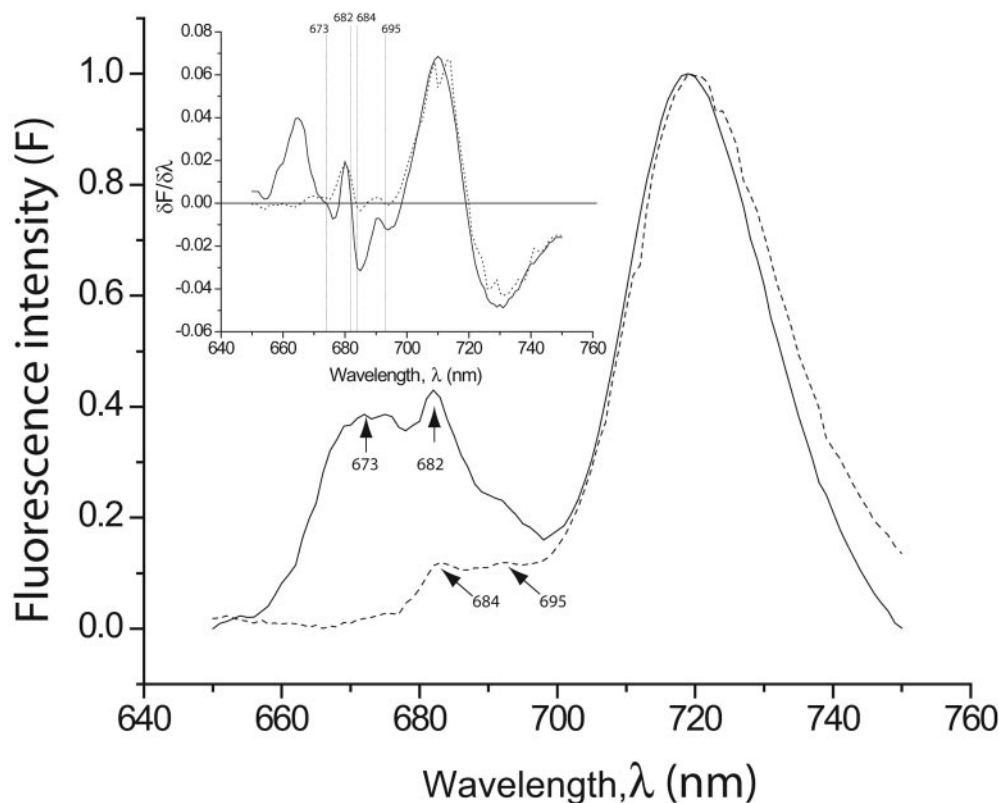


FIG. 2. 77 K fluorescence spectra of isolated thylakoid and plasma membranes. 77 K fluorescence was measured with excitation at 420 ± 5 nm. Solid line, PM; dashed line, TM. Fluorescence intensities (F) were normalized to the emission intensity at 720 nm. Inset, first derivative of the spectra used for assigning peak positions. Peak positions are noted by the gray dotted lines (inset) and arrows.

higher fluorescence levels than TM (Fig. 3A). High chlorophyll fluorescence has been shown to indicate a partially active PSII (15). The rise time of chlorophyll fluorescence in PM was much faster than in TM (Fig. 3B and Table I). However, it was still significantly slower than the rise time of extracted chlorophyll in methanol (Fig. 3B). The area above the induction curve, which serves as a measure of the overall rate of fluorescence induction, was 85 ± 9 area units (absorbance units) for PM, whereas the area above the induction curve of extracted chlorophyll was only 40 ± 14 absorbance units ($n = 3$; see Table I for details). A t test performed on these values indicates that the difference between the two is statistically significant, with a $p < 0.05$ value. These data show that excitation transfer and charge separation activities take place in PSII complexes in PM, albeit to a smaller extent than in TM.

Only after the addition of the PSII inhibitor DCMU did the rise time of TM resemble that of PM (Fig. 3). DCMU binds to the Q_B site of PSII and inhibits electron transfer to the plastoquinone pool (16). In addition, fluorescence induction rates in TM were inversely correlated to the actinic light intensity,

whereas induction rates in PM were uncorrelated (data not shown). The addition of up to $40 \mu\text{M}$ artificial PSII acceptor 2,6-dichloro-*p*-benzoquinone did not affect the fluorescence rise kinetics (data not shown).

To examine the PSII acceptor side we tested the DCMU binding properties of purified membrane fractions. Both membrane fractions were able to bind ^{14}C -labeled DCMU (Table I). The bound [14 C]DCMU was displaced by an excess of cold DCMU or atrazine. Calculating the fraction of tightly bound DCMU from the difference between total and free [14 C]DCMU indicates that the binding properties of TM and PM were similar (Table I). Similar data were recorded when cold atrazine was used to displace [14 C]DCMU (data not shown). A more comprehensive analysis of the binding constants and the number of sites per chlorophyll could not be performed due to the large amount of membranes required (3 liters of culture processed for each experiment). Nevertheless, the data presented here demonstrate the existence of an assembled Q_B site on the acceptor side of PM PSII.

The water splitting activity on the donor side of PSII relies

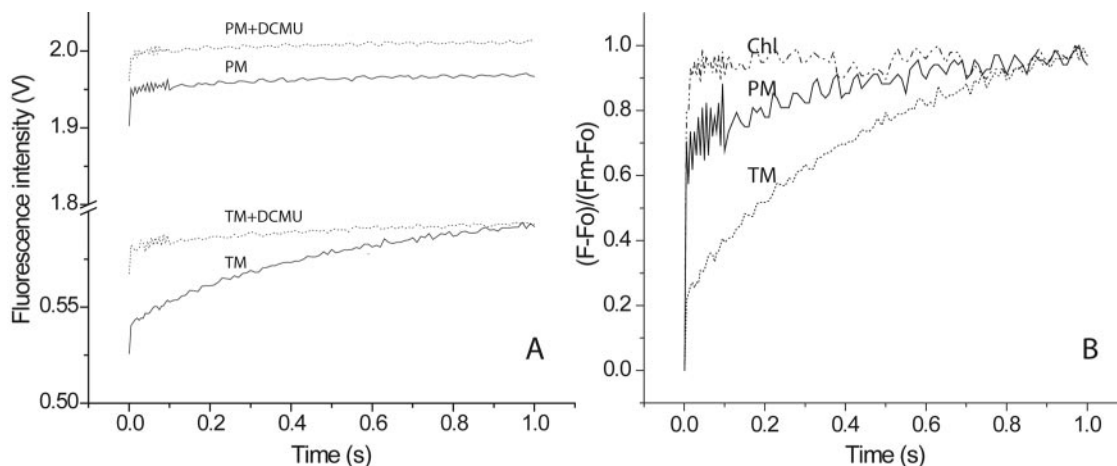
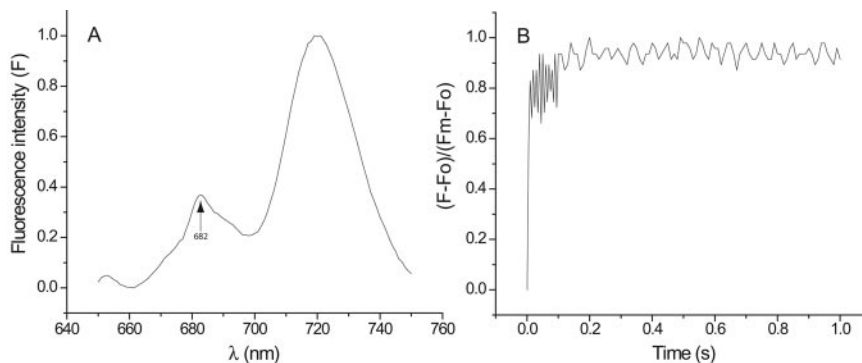


FIG. 3. **Kinetics of chlorophyll fluorescence.** A, chlorophyll fluorescence induction of 3 min of dark-adapted PM and TM in the absence and presence of $5 \mu\text{M}$ DCMU. B, normalized fluorescence kinetics of TM, PM, and methanol-extracted Chl without DCMU. All samples were measured at an equal $16 \mu\text{g/ml}$ Chl concentration. F_o , initial fluorescence intensity; F_m , maximum fluorescence intensity; V, volts.

FIG. 4. **Fluorescence measurements on $\Delta ctpA$ mutant cells.** A, fluorescence excitation spectra of $\Delta ctpA$ total membranes (excitation at $420 \pm 5 \text{ nm}$). Fluorescence intensity (F) was normalized to the emission intensity at 720 nm . The 682 nm peak position is noted by an arrow. B, normalized chlorophyll fluorescence kinetics of $\Delta ctpA$ total membranes ($16 \mu\text{g Chl/ml}$) without DCMU.



on the assembly of the manganese cluster. Our measurements indicate that manganese ions are present in both PM and TM (Table I). The higher manganese concentration detected in the PM is in agreement with our previous study that identified a large manganese pool in the periplasmic space of *Synechocystis* 6803 cells (17). Therefore, manganese limitation cannot be the cause of the restriction on electron transfer rates in PM-localized PSII. Furthermore, the addition of up to 5 mM external MnCl_2 did not affect the fluorescence rise kinetics of PM (data not shown).

Taken together, the properties of PSII in purified PM indicate that the donor side is inactive. Therefore, it is of interest to compare them to the properties of PSII in an established donor side-inactivated mutant. The $\Delta ctpA$ strain, in which the gene coding for the pD1-processing enzyme is disrupted (18), is such a mutant. A recent study of PSII complexes isolated from this mutant demonstrates that manganese cannot bind to PSII containing the unprocessed pD1 protein (7). $\Delta ctpA$ cells are both heterotrophic and light-sensitive. Consequently, it is difficult to produce the total membrane mass required for membrane fractionation. Therefore, the analysis was performed on total membranes. $\Delta ctpA$ membranes display a number of striking similarities to PSII in the plasma membrane. In the fluorescence spectra, a peak at 682 nm was detected (Fig. 4A). The ratio of $682/695\text{-nm}$ fluorescence in $\Delta ctpA$ membranes was 1.44, similar to that in PM (Table I). In addition, a shoulder in the 670-nm region of the spectrum was also observed (Fig. 4A). The fluorescence induction kinetics of $\Delta ctpA$ membranes were similar to those of PM with an area above the curve of 73 absorbance units (Fig. 4B). Also, the addition of DCMU had no effect on the fluorescence kinetics (data not shown). Like PM, the overall fluorescence intensity was 4.5 times higher than TM on an equal chlorophyll basis.

DISCUSSION

Assembly of PSII is a complex process including not only the recruitment of protein subunits at an exact stoichiometric ratio but also the insertion and activation of redox active cofactors. In previous work we found an assembled PSII complex in the PM (8). Because active photosynthesis occurs in the TM we have proposed that the core subunits D1, D2, and cytochrome b_{559} are assembled in the PM, and the CP43 and CP47 subunits are added in the TM (8). During this work we studied the activity of PSII complexes in PM and TM to reconstruct the pathway of cofactor assembly and activation.

The PSII centers in PM exhibited fluorescence characteristics similar to those observed in PSII core complexes (13). These include blue-shifted fluorescence peaks (Fig. 2) and fast fluorescence rise times (Fig. 3). TM membranes, on the other hand, exhibit much slower fluorescence rise kinetics. The fluorescence induction kinetics of TM indicated the ability of PSII in these membranes to undergo multiple turnovers, whereas the PSII in PM cannot. However, since the fluorescence rise kinetics of the PSII centers in PM were significantly slower than those of extracted chlorophyll, it is evident that the PSII in PM was capable of excitation transfer and primary charge separation.

The inability of PSII in PM to perform multiple turnovers could be the result of either an unassembled donor side and/or of an unassembled acceptor side of PSII. The herbicide binding experiments indicate the existence of a functional Q_B site in PM, suggesting that the limitation is not on the acceptor side, and therefore, it is most probably on the donor side. Additional evidence for an unassembled donor side can be found in the comparison between PM and $\Delta ctpA$ membranes. The fluores-

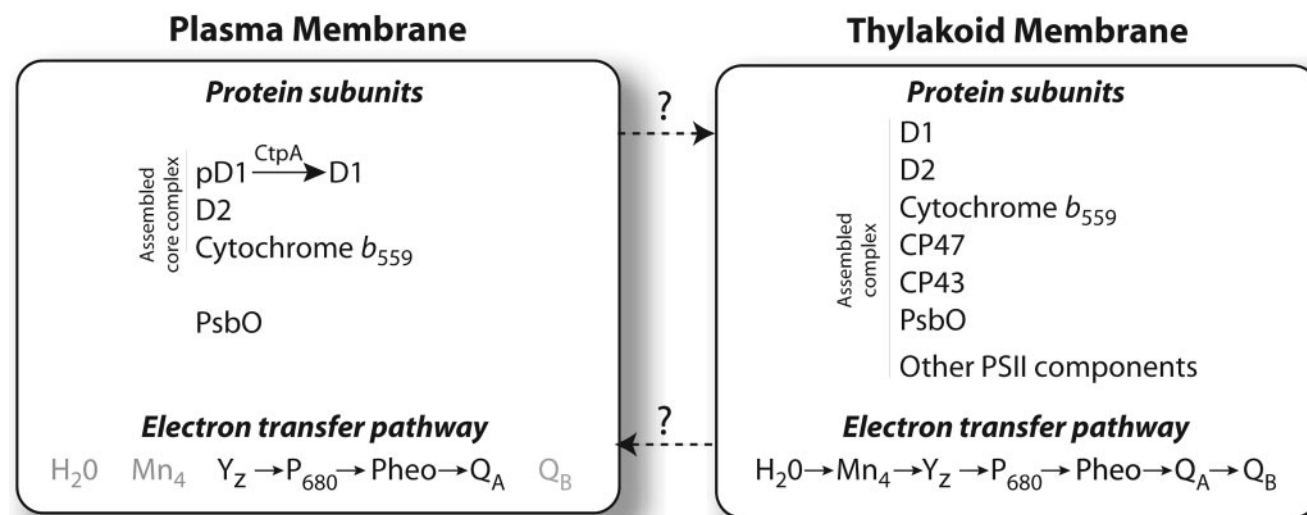


FIG. 5. **Proposed topological model for PSII biogenesis events in *Synechocystis* 6803.** See “Discussion” for further details. *Pheo*, pheophytin.

cence spectrum and rise kinetic parameters measured in membranes isolated from this donor side-inactive mutant are very similar those measured in PM.

In the absence of a manganese cluster, free manganese is able to donate electrons to fully assembled PSII complexes that were stripped from their manganese cluster (19). This, however, is not the case in PM-localized PSII in which even the addition of extra manganese did not affect the fluorescence rise kinetics of PM. Importantly, previous studies show that the CP43 protein, which contributes ligands to the manganese cluster (2), is found exclusively in TM (8). Without the contribution of the CP43 ligands the assembly of a manganese complex is highly unlikely.

An inactive manganese cluster on the donor side of PSII has additional effects on the acceptor side. In the absence of D1 processing or after the removal of manganese or calcium ions from the donor side of PSII, the Q_A/Q_A^- midpoint potential is upshifted by ~ 150 mV (20, 21). As a result, electron transfer from Q_A to Q_B is blocked. This explains the inability of PM-localized PSII to transfer electrons to the artificial acceptor 2,6-dichloro-*p*-benzoquinone despite the observation that the Q_B site is functionally assembled.

Based on these results we propose the following topological model for the assembly pathway of PSII (Fig. 5). First, the reaction center core is assembled in the PM. This core includes the pD1/D1, D2, and cytochrome b_{559} proteins. The same proteins were detected in the initial assembly steps of higher plant PSII (22). This PSII core protein complex contains the P_{680} chlorophyll assembly and correctly folded Q_A and Q_B quinone binding sites. The second step in PSII assembly is the processing of pD1 by the CtpA protease. The processing of pD1 is necessary but not sufficient for the assembly of the manganese cluster (7). Next, the PSII core complex is transported to the TM. The mechanism by which this occurs is still unknown. Neither physical contacts nor transport vesicles between PM and TM have been detected in *Synechocystis* 6803 (23).

Only after the transfer of the core complex into the TM and the recruitment of the CP43 protein can the manganese cluster form. After the assembly of the manganese cluster in the TM, it is stabilized by the binding of the extrinsic manganese-stabilizing proteins, PsbO/U/V/P/Q (3). PsbO was detected in both PM and TM (8), but in the absence of an assembled manganese cluster it does not bind to the PSII complex (7).

Incorporation of the CP47 protein as well as a number of other smaller integral membrane proteins completes the assembly of a fully functional PSII. Such a stepwise process separates assembly from activity and ensures that PSII complexes will be photochemically active only in the TM. This separation can protect the photosynthetic apparatus from partial electron transfer reactions that can result in the generation of harmful radical species.

In the course of its normal function in TM, PSII can be photodamaged by the redox reactions it performs (4). As a result, the D1 protein is degraded and must be replaced. For this process to take place in a cyanobacterial cell, the core D2 and cytochrome b_{559} proteins must detach from the damaged complex and be transported back to the PM, where a new pD1 protein will be inserted. As in the case of transfer of assembled core complexes from PM to TM, the mechanism by which this transport process occurs is unknown. Coupling PSII biogenesis to the topology of the membrane systems in *Synechocystis* 6803 will be central to the understanding of the dynamics of the photosynthetic apparatus in these cyanobacterial cells.

Acknowledgments—We thank other members of the Pakrasi laboratory for collegial discussions.

REFERENCES

- Goussias, C., Boussac, A., and Rutherford, A. W. (2002) *Philos. Trans. R. Soc. Lond. B. Biol. Sci.* **357**, 1369–1381
- Ferreira, K. N., Iverson, T. M., Maghlaoui, K., Barber, J., and Iwata, S. (2004) *Science* **303**, 1831–1838
- Thornton, L. E., Ohkawa, H., Roose, J. L., Kashino, Y., Keren, N., and Pakrasi, H. B. (2004) *Plant Cell* **16**, 2164–2175
- Keren, N., and Ohad, I. (1998) in *The Molecular Biology of Chloroplast and Mitochondria in Chlamydomonas* (Rocaix, J. D., Goldschmidt-Clermont, M., and Merchant, S., eds) pp. 569–596, Kluwer Academic Publishers Group, Dordrecht, Netherlands
- Keren, N., Berg, A., van Kan, P. J., Levanon, H., and Ohad, I. I. (1997) *Proc. Natl. Acad. Sci. U. S. A.* **94**, 1579–1584
- Choquet, Y., Wostrickoff, K., Rimbault, B., Zito, F., Girard-Bascou, J., Drapier, D., and Wollman, F. A. (2001) *Biochem. Soc. Trans.* **29**, 421–426
- Roose, J. L., and Pakrasi, H. B. (2004) *J. Biol. Chem.* **279**, 45417–45422
- Zak, E., Norling, B., Maitra, R., Huang, F., Andersson, B., and Pakrasi, H. B. (2001) *Proc. Natl. Acad. Sci. U. S. A.* **98**, 13443–13448
- Allen, M. M. (1968) *J. Phycol.* **4**, 1–4
- Norling, B., Zak, E., Andersson, B., and Pakrasi, H. (1998) *FEBS Lett.* **436**, 189–192
- Arnon, D. I. (1949) *Plant Physiol.* **24**, 1–15
- Lind, L. K., Shukla, V. K., Nyhus, K. J., and Pakrasi, H. B. (1993) *J. Biol. Chem.* **268**, 1575–1579
- Seibert, M., Picorel, R., Rubin, A. B., and Connolly, J. S. (1988) *Plant Physiol.* **87**, 303–306
- Schreiber, U., and Krieger, A. (1996) *FEBS Lett.* **397**, 131–135

15. Bennoun, P., and Delepelaire, P. (1982) in *Methods in Chloroplast Biology* (Edelman, M., Hallick, R. B., and Chua, N.-H., eds) pp. 25–38, Elsevier Science Publishers B. V., Amsterdam
16. Bishop, N. I. (1958) *Biochim. Biophys. Acta* **27**, 205–206
17. Keren, N., Kidd, M. J., Penner-Hahn, J. E., and Pakrasi, H. B. (2002) *Biochemistry* **41**, 15085–15092
18. Anbudurai, P. R., Mor, T. S., Ohad, I., Shestakov, S. V., and Pakrasi, H. B. (1994) *Proc. Natl. Acad. Sci. U. S. A.* **91**, 8082–8086
19. Babcock, G. T., and Sauer, K. (1975) *Biochim. Biophys. Acta* **396**, 48–62
20. Johnson, G. N., Rutherford, A. W., and Krieger, A. (1995) *Biochim. Biophys. Acta* **1229**, 202–207
21. Krieger, A., Rutherford, A. W., and Johnson, G. N. (1995) *Biochim. Biophys. Acta* **1229**, 193–201
22. van Wijk, K. J., Roobol-Boza, M., Kettunen, R., Andersson, B., and Aro, E. M. (1997) *Biochemistry* **36**, 6178–6186
23. Spence, E., Sarcina, M., Ray, N., Moller, S. G., Mullineaux, C. W., and Robinson, C. (2003) *Mol. Microbiol.* **48**, 1481–1489